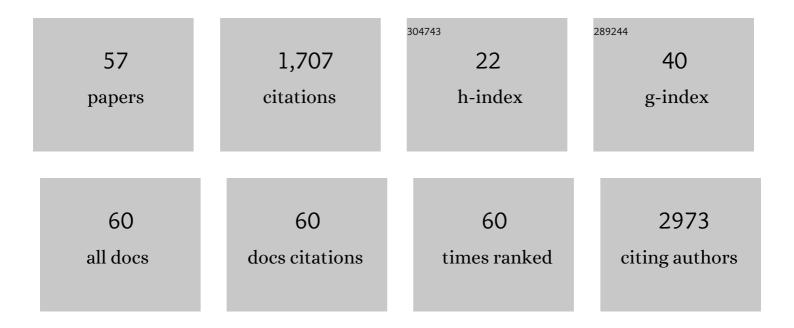
Emanuele Smecca

List of Publications by Year in descending order

Source: https://exaly.com/author-pdf/6676787/publications.pdf Version: 2024-02-01



#	Article	IF	CITATIONS
1	Black‥ellow Bandgap Tradeâ€Off During Thermal Stability Tests in Lowâ€Temperature Euâ€Doped CsPbl ₃ . Solar Rrl, 2022, 6, .	5.8	8
2	Outâ€ofâ€Glovebox Integration of Recyclable Europiumâ€Doped CsPbI ₃ in Tripleâ€Mesoscopic Carbonâ€Based Solar Cells Exceeding 9% Efficiency. Solar Rrl, 2022, 6, .	5.8	9
3	Two-step MAPbI ₃ deposition by low-vacuum proximity-space-effusion for high-efficiency inverted semitransparent perovskite solar cells. Journal of Materials Chemistry A, 2021, 9, 16456-16469.	10.3	25
4	CsPbBr ₃ , MAPbBr ₃ , and FAPbBr ₃ Bromide Perovskite Single Crystals: Interband Critical Points under Dry N ₂ and Optical Degradation under Humid Air. Journal of Physical Chemistry C, 2021, 125, 4938-4945.	3.1	26
5	Optical behaviour of γ-black CsPbl ₃ phases formed by quenching from 80 °C and 325 °C. JPhys Materials, 2021, 4, 034011.	4.2	6
6	Formation of CsPbI ₃ γâ€Phase at 80 °C by Europiumâ€Assisted Snowplow Effect. Advanced Energy and Sustainability Research, 2021, 2, 2100091.	5.8	8
7	Exploring the Structural Competition between the Black and the Yellow Phase of CsPbI3. Nanomaterials, 2021, 11, 1282.	4.1	12
8	MAPbI3 Deposition by LV-PSE on TiO2 for Photovoltaic Application. Frontiers in Electronics, 2021, 2, .	3.2	1
9	Ni/4H-SiC interaction and silicide formation under excimer laser annealing for ohmic contact. Materialia, 2020, 9, 100528.	2.7	12
10	Improved Electrical and Structural Stability in HTL-Free Perovskite Solar Cells by Vacuum Curing Treatment. Energies, 2020, 13, 3953.	3.1	7
11	Temperature-Dependent Optical Band Gap in CsPbBr ₃ , MAPbBr ₃ , and FAPbBr ₃ Single Crystals. Journal of Physical Chemistry Letters, 2020, 11, 2490-2496.	4.6	173
12	Local Order and Rotational Dynamics in Mixed A-Cation Lead Iodide Perovskites. Journal of Physical Chemistry Letters, 2020, 11, 1068-1074.	4.6	31
13	Full Efficiency Recovery in Hole-Transporting Layer-Free Perovskite Solar Cells With Free-Standing Dry-Carbon Top-Contacts. Frontiers in Chemistry, 2020, 8, 200.	3.6	8
14	Nanostructured TiO ₂ Grown by Low-Temperature Reactive Sputtering for Planar Perovskite Solar Cells. ACS Applied Energy Materials, 2019, 2, 6218-6229.	5.1	27
15	New Synthetic Route for the Growth of α-FeOOH/NH ₂ -Mil-101 Films on Copper Foil for High Surface Area Electrodes. ACS Omega, 2019, 4, 18495-18501.	3.5	8
16	Bimodal Porosity and Stability of a TiO2 Gig-Lox Sponge Infiltrated with Methyl-Ammonium Lead Iodide Perovskite. Nanomaterials, 2019, 9, 1300.	4.1	7
17	Pb clustering and PbI2 nanofragmentation during methylammonium lead iodide perovskite degradation. Nature Communications, 2019, 10, 2196.	12.8	116
18	Porous Gig-Lox TiO2 Doped with N2 at Room Temperature for P-Type Response to Ethanol. Chemosensors, 2019, 7, 12.	3.6	4

Emanuele Smecca

#	Article	IF	CITATIONS
19	Properties of Al2O3 thin films deposited on 4H-SiC by reactive ion sputtering. Materials Science in Semiconductor Processing, 2019, 93, 290-294.	4.0	10
20	Morphological and electrical properties of Nickel based Ohmic contacts formed by laser annealing process on n-type 4H-SiC. Materials Science in Semiconductor Processing, 2019, 97, 62-66.	4.0	25
21	Nitrogen doped spongy TiO2 layers for sensors application. Materials Science in Semiconductor Processing, 2019, 98, 44-48.	4.0	8
22	Nitrogen Soaking Promotes Lattice Recovery inÂPolycrystalline Hybrid Perovskites. Advanced Energy Materials, 2019, 9, 1803450.	19.5	46
23	Heterogeneous growth of continuous ZIF-8 films on low-temperature amorphous silicon. Applied Surface Science, 2019, 473, 182-189.	6.1	7
24	Simulation of the Growth Kinetics in Group IV Compound Semiconductors. Physica Status Solidi (A) Applications and Materials Science, 2019, 216, 1800597.	1.8	6
25	Innovative spongy TiO2 layers for gas detection at low working temperature. Sensors and Actuators B: Chemical, 2018, 259, 658-667.	7.8	23
26	Stability and Degradation in Hybrid Perovskites: Is the Glass Half-Empty or Half-Full?. Journal of Physical Chemistry Letters, 2018, 9, 3000-3007.	4.6	102
27	Revealing a Discontinuity in the Degradation Behavior of CH ₃ NH ₃ Pbl ₃ during Thermal Operation. Journal of Physical Chemistry C, 2017, 121, 13577-13585.	3.1	37
28	First Evidence of CH ₃ NH ₃ Pbl ₃ Optical Constants Improvement in a N ₂ Environment in the Range 40–80 °C. Journal of Physical Chemistry C, 2017, 121, 7703-7710.	3.1	49
29	Pervasive infiltration and multi-branch chemisorption of N-719 molecules into newly designed spongy TiO ₂ layers deposited by gig-lox sputtering processes. Journal of Materials Chemistry A, 2017, 5, 25529-25538.	10.3	12
30	Performance of natural-dye-sensitized solar cells by ZnO nanorod and nanowall enhanced photoelectrodes. Beilstein Journal of Nanotechnology, 2017, 8, 287-295.	2.8	21
31	Influence of hydrofluoric acid treatment on electroless deposition of Au clusters. Beilstein Journal of Nanotechnology, 2017, 8, 183-189.	2.8	8
32	Controlled Al3+ Incorporation in the ZnO Lattice at 188 °C by Soft Reactive Co-Sputtering for Transparent Conductive Oxides. Energies, 2016, 9, 433.	3.1	9
33	Multi-Scale-Porosity TiO2 scaffolds grown by innovative sputtering methods for high throughput hybrid photovoltaics. Scientific Reports, 2016, 6, 39509.	3.3	34
34	Spontaneous bidirectional ordering of CH3NH3+ in lead iodide perovskites at room temperature: The origins of the tetragonal phase. Scientific Reports, 2016, 6, 24443.	3.3	37
35	Stability of solution-processed MAPbI ₃ and FAPbI ₃ layers. Physical Chemistry Chemical Physics, 2016, 18, 13413-13422. Structural and electronic transitions in Animilimath	2.8	208
36	<pre>xmlns:mml="http://www.w3.org/1998/Math/MathML"><mml:mrow><mml:mi mathvariant="normal">G</mml:mi><mml:msub><mml:mi mathvariant="normal">e</mml:mi><mml:mn>2</mml:mn></mml:msub><mml:mi mathvariant="normal">S</mml:mi><mml:msub><mml:mi mathvariant="normal">>S</mml:mi><mml:msub><mml:mi mathvariant="normal">>S</mml:mi><mml:msub><mml:mi mathvariant="normal">>></mml:mi><mml:msub><mml:mi mathvariant="normal">>></mml:mi><mml:msub><mml:mi mathvariant="normal">>></mml:mi><mml:msub><mml:mi mathvariant="normal">>></mml:mi><mml:msub><mml:mi mathvariant="normal">>></mml:mi><mml:msub><mml:mi mathvariant="normal">>></mml:mi><mml:msub><mml:mi mathvariant="normal">>></mml:mi><mml:mn>2</mml:mn></mml:msub><mml:mi mathvariant="normal">>></mml:mi></mml:msub><mml:mi mathvariant="normal">>></mml:mi></mml:msub></mml:msub><mml:mi mathvariant="normal">>></mml:mi></mml:msub></mml:msub></mml:msub>>></mml:msub></mml:msub></mml:mrow></pre>	3.2	33

Emanuele Smecca

#	Article	IF	CITATIONS
37	From Pbl ₂ to MAPbl ₃ through Layered Intermediates. Journal of Physical Chemistry C, 2016, 120, 19768-19777.	3.1	26
38	Phase Transitions in Ge-Sb-Te Alloys Induced by Ion Irradiations. MRS Advances, 2016, 1, 2701-2709.	0.9	2
39	A Comparison Among Low Temperature Piezoelectric Flexible Sensors Based on Polysilicon TFTs for Advanced Tactile Sensing on Plastic. Journal of Display Technology, 2016, 12, 209-213.	1.2	12
40	Metalâ€Organic Chemical Vapor Deposition (MOCVD) Synthesis of Heteroepitaxial Pr _{0.7} Ca _{0.3} MnO ₃ Films: Effects of Processing Conditions on Structural/Morphological and Functional Properties. ChemistryOpen, 2015, 4, 523-532.	1.9	10
41	Similar Structural Dynamics for the Degradation of CH ₃ NH ₃ PbI ₃ in Air and in Vacuum. ChemPhysChem, 2015, 16, 3064-3071.	2.1	80
42	Atomistic origins of CH3NH3PbI3 degradation to PbI2 in vacuum. Applied Physics Letters, 2015, 106, .	3.3	158
43	Low-cost high-haze films based on ZnO nanorods for light scattering in thin c-Si solar cells. Applied Physics Letters, 2015, 106, .	3.3	21
44	Texture of MAPbI ₃ Layers Assisted by Chloride on Flat TiO ₂ Substrates. Journal of Physical Chemistry C, 2015, 119, 19808-19816.	3.1	36
45	AlN texturing and piezoelectricity on flexible substrates for sensor applications. Applied Physics Letters, 2015, 106, .	3.3	33
46	Low temperature sputtered TiO ₂ nano sheaths on electrospun PES fibers as high porosity photoactive material. RSC Advances, 2015, 5, 73444-73450.	3.6	14
47	Spatially Confined Functionalization of Transparent NiO Thin Films with a Luminescent (1,10â€Phenanthroline)tris(2â€thenoyltrifluoroacetonato)europium Monolayer. European Journal of Inorganic Chemistry, 2015, 2015, 1261-1268.	2.0	7
48	Low-temperature flexible piezoelectric AlN capacitor integrated on ultra-flexible poly-Si TFT for advanced tactile sensing. , 2014, , .		2
49	Tetra-anionic porphyrin loading onto ZnO nanoneedles: A hybrid covalent/non covalent approach. Materials Chemistry and Physics, 2014, 143, 977-982.	4.0	6
50	A strategy to stabilise the local structure of Ti4+ and Zn2+ species against aging in TiO2/aluminium-doped ZnO bi-layers for applications in hybrid solar cells. Journal of Applied Physics, 2014, 116, .	2.5	5
51	Piezoelectric domains in BiFeO3 films grown via MOCVD: Structure/property relationship. Surface and Coatings Technology, 2013, 230, 168-173.	4.8	12
52	Spectroscopic and Theoretical Study of the Grafting Modes of Phosphonic Acids on ZnO Nanorods. Journal of Physical Chemistry C, 2013, 117, 5364-5372.	3.1	45
53	Improvement of the fatigue resistance of NiTi endodontic files by surface and bulk modifications. International Endodontic Journal, 2010, 43, 866-873.	5.0	37
54	Engineered Si(100) surfaces for the gas-phase anchoring of metal β-diketonate complexes. Inorganica Chimica Acta, 2007, 360, 170-178.	2.4	19

#	Article	IF	CITATIONS
55	Metal/P-GaN Contacts on AlGaN/GaN Heterostructures for Normally-Off HEMTs. Materials Science Forum, 0, 858, 1170-1173.	0.3	7
56	High Resolution Investigation of Stacking Fault Density by HRXRD and STEM. Materials Science Forum, 0, 963, 346-349.	0.3	5
57	Structural and Electrical Characterization of Ni-Based Ohmic Contacts on 4H-SiC Formed by Solid-State Laser Annealing. Materials Science Forum, 0, 1062, 417-421.	0.3	2